A new bound on excess frequency noise in second harmonic generation in PPKTP at the 10^{-19} level

D. Yeaton-Massey[1,*] **and R. X. Adhikari**[1]

[1] *California Institute of Technology, Division of Physics, Math, and Astronomy Pasadena, CA, 91125, USA*

[*] *davidym@caltech.edu*

Abstract: We report a bound on the relative frequency fluctuations in nonlinear second harmonic generation. A 1064 nm Nd:YAG laser is used to read out the phase of a Mach-Zehnder interferometer while PPKTP, a nonlinear crystal, is placed in each arm to generate second harmonic light. By comparing the arm length difference of the Mach Zehnder as read out by the fundamental 1064 nm light, and its second harmonic at 532 nm, we can bound the excess frequency noise introduced in the harmonic generation process. We report an amplitude spectral density of frequency noise with total RMS frequency deviation of 3 mHz and a minimum value of 20 $\mu\mathrm{Hz}/\mathrm{Hz}^{1/2}$ over 250 seconds with a measurement bandwidth of 128 Hz, corresponding to an Allan deviation of 10^{-19} at 20 seconds.

OCIS codes: (190.2620) Harmonic generation and mixing; (120.2920) Homodyning; (120.3180) Interferometry.

References and links

1. J. A. Armstrong, N. Bloembergen, J. Ducuing, and P. S. Pershan, "Interactions between Light Waves in a Nonlinear Dielectric," Phys. Rev. **127**, 1918–1939 (1962).
2. J. Stenger, H. Schnatz, C. Tamm, and H. R. Telle, "Ultraprecise Measurement of Optical Frequency Ratios," Phys. Rev. Lett. **88**, 073601 (2002).
3. E. J. Zang, J. P. Cao, Y. Li, C. Y. Li, Y. K. Deng, and C. Q. Gao, "Realization of Four-Pass I_2 Absorption Cell in 532-nm Optical Frequency Standard," IEEE transactions on Instrumentation and Measurement **56**, 673–676 (2007).
4. G. Grosche, B. Lipphardt, and H. Schnatz, "Optical frequency synthesis and measurement using fibre-based femtosecond lasers," The European Physical Journal D - Atomic, Molecular, Optical and Plasma Physics **48**, 27–33 (2008).
5. I. Coddington, W. C. Swann, L. Lorini, J. C. Bergquist, Y. Le Coq, C. W. Oates, Q. Quraishi, K. S. Feder, J. W. Nicholson, P. S. Westbrook, S. A. Diddams, and N. R. Newbury, "Coherent optical link over hundreds of metres and hundreds of terahertz with subfemtosecond timing jitter," Nature Photonics **1**, 283–287 (2007).
6. T. Rosenband, D. B. Hume, P. O. Schmidt, C. W. Chou, A. Brusch, L. Lorini, W. H. Oskay, R. E. Drullinger, T. M. Fortier, J. E. Stalnaker, S. A. Diddams, W. C. Swann, N. R. Newbury, W. M. Itano, D. J. Wineland, and J. C. Bergquist, "Frequency Ratio of Al^+ and Hg^+ Single-Ion Optical Clocks; Metrology at the 17th Decimal Place," Science **319**, 1808–1812 (2008).
7. T. M. Fortier, N. Ashby, J. C. Bergquist, M. J. Delaney, S. A. Diddams, T. P. Heavner, L. Hollberg, W. M. Itano, S. R. Jefferts, K. Kim, F. Levi, L. Lorini, W. H. Oskay, T. E. Parker, J. Shirley, and J. E. Stalnaker, "Precision Atomic Spectroscopy for Improved Limits on Variation of the Fine Structure Constant and Local Position Invariance," Phys. Rev. Lett. **98**, 070801 (2007).
8. LIGO Scientific Collaboration, "LIGO: the Laser Interferometer Gravitational-Wave Observatory," Reports on Progress in Physics **72**, 076901 (2009).

9. A. J. Mullavey, B. J. J. Slagmolen, J. Miller, M. Evans, P. Fritschel, D. Sigg, S. J. Waldman, D. A. Shaddock, and D. E. McClelland, "Arm-length stabilisation for interferometric gravitational-wave detectors using frequency-doubled auxiliary lasers," Optics Express **20**, 81–89 (2012).
10. K. Izumi, K. Arai, B. Barr, J. Betzwieser, A. Brooks, K. Dahl, S. Doravari, J. C. Driggers, W. Z. Korth, H. Miao, J. Rollins, S. Vass, D. Yeaton-Massey, R. X. Adhikari, "Multi-wavelength cavity metrology," arXiv:1205.1257 (2012)
11. F. Khalili, S. Danilishin, H. Müller-Ebhardt, H. Miao, Y. Chen, and C. Zhao, "Negative optical inertia for enhancing the sensitivity of future gravitational-wave detectors," Phys. Rev. D **83**, 062003 (2011).
12. B. Willke, N. Uehara, E. K. Gustafson, R. L. Byer, P. J. King, S. U. Seel, and J. R. L. Savage, "Spatial and temporal filtering of a 10-w nd:yag laser with a fabry–perot ring-cavity premode cleaner," Opt. Lett. **23**, 1704–1706 (1998).
13. V. Leonhardt and J. B. Camp, "Space interferometry application of laser frequency stabilization with molecular iodine," Appl. Opt. **45**, 4142–4146 (2006).
14. Y. Levin, "Fluctuation–dissipation theorem for thermo-refractive noise," Physics Letters A **372**, 1941–1944 (2007).
15. D. Heinert, A. G. Gurkovsky, R. Nawrodt, S. P. Vyatchanin, and K. Yamamoto, "Thermorefractive noise of finite-sized cylindrical test masses," Phys. Rev. D **84**, 062001 (2011).
16. L.-S. Ma, Z. Bi, A. Bartels, L. Robertsson, M. Zucco, R. S. Windeler, G. Wilpers, C. Oates, L. Hollberg, and S. A. Diddams, "Optical Frequency Synthesis and Comparison with Uncertainty at the 10^{-19} Level," Science **303**, 1843–1845 (2004).
17. L. Robertsson, "International comparison of $^{127}I_2$-stabilized frequency-doubled Nd:YAG lasers between the BIPM, the NRLM and the BNM-INM," Metrologia **38** (2001).
18. J. E. Stalnaker, S. A. Diddams, T. M. Fortier, K. Kim, L. Hollberg, J. C. Bergquist, W. M. Itano, M. J. Delany, L. Lorini, W. H. Oskay, T. P. Heavner, S. R. Jefferts, F. Levi, T. E. Parker, and J. Shirley, "Optical-to-microwave frequency comparison with fractional uncertainty of 10^{-15}," Applied Physics B: Lasers and Optics **89**, 167–176 (2007).
19. Rubiola, *Phase Noise and Frequency Stability in Oscillators* (Cambridge University Press, 2008).
20. I. R. C. Committee, "Characterization of Frequency and Phase Noise," Report (1986).
21. O. Terra, G. Grosche, K. Predehl, R. Holzwarth, T. Legero, U. Sterr, B. Lipphardt, and H. Schnatz, "Phase-coherent comparison of two optical frequency standards over 146 km using a telecommunication fiber link," Applied Physics B: Lasers and Optics **97**, 541–551 (2009). 10.1007/s00340-009-3653-2.

1. Introduction

Harmonic generation of optical fields in nonlinear optical crystals can be modeled with classical coupled wave equations [1]. Define the fundamental and second harmonic fields as $E_1 = \mathscr{E}_1 \exp(2\pi i \nu_1 t)$ and $E_2 = \mathscr{E}_2 \exp(2\pi i \nu_2 t)$, respectively. In ideal second harmonic generation, $\nu_2 = 2\nu_1$. While this frequency ratio has been measured very precisely ($\langle \nu_2/\nu_1 \rangle = 7 \times 10^{-19}$ [2]), we present a lower bound to the frequency noise, or the spectrum of the time dependent quantity $\nu_2 - 2\nu_1$.

Several experiments at the forefront of precision metrology and frequency standards use harmonic generation in their experiments. These include iodine stabilized Nd:YAG lasers [3], optical frequency combs [4, 5], measurement of optical frequency ratios [2, 6], and precision atomic spectroscopy [7]. Many of these experiments provide bounds to any excess frequency noise which might be found in the second harmonic generation (SHG) process (e.g. from thermodynamic fluctuations in the crystal temperature). As experiments like these push towards lower noise levels, the fundamental noise sources in second harmonic generation may become a relevant noise source.

Another field which utilizes precision SHG is interferometric detection of gravitational waves. These interferometers require measurements of mirror displacements at the level of $10^{-20}\,\mathrm{m}/\sqrt{\mathrm{Hz}}$ [8]. To achieve such high precision, these interferometers use seismically isolated suspended mirrors which make up multiple coupled optical cavities with narrow linewidths. It has proven challenging to control these cavities and bring them simultaneously into resonance. In order to simplify this problem, auxiliary fields will be generated by SHG and used to form independent signals for two of the cavities. This technique is being developed using some small scale prototypes [9, 10]. To understand the limits of such a scheme, we need to

bound the frequency noise introduced in the second harmonic generation process. In our case, we use a 1064 nm carrier (Nd:YAG), and generate the 532 nm doubled light with PPKTP crystals. In order to meet the stability requirements for this technique, the excess frequency noise must be less than 70 mHz RMS from 10 mHz to 30 Hz [9]. In the future, optical configurations using more than one wavelength inside the interferometer to beat standard quantum noise limits of the detection [11] may be used. Fundamental noise limits in harmonic generation may be relevant there.

2. Experimental Setup

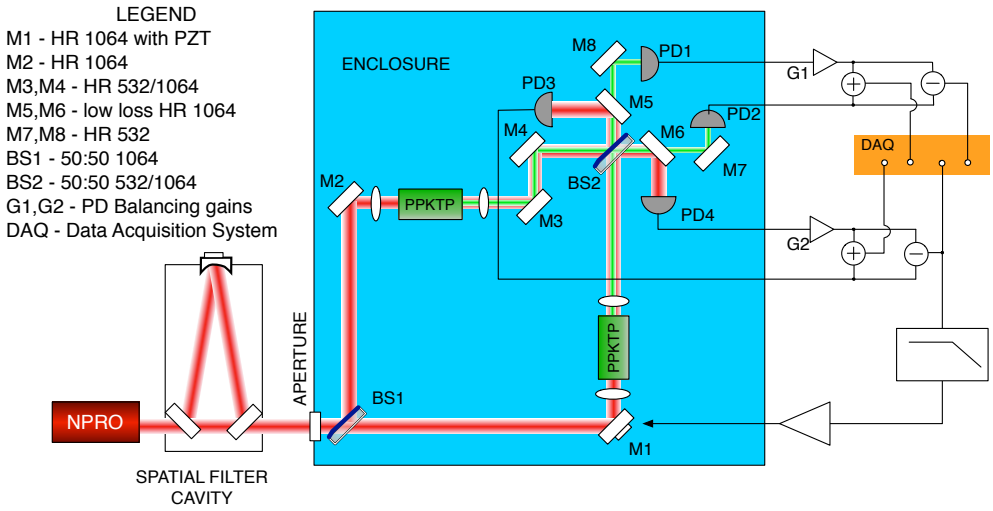

Fig. 1. Experimental layout - A dual wavelength Mach-Zehnder Interferometer. Some readout mirrors for harmonic separation are not shown. See text for a more complete description.

Figure 1 shows the experimental setup used to measure the uncorrelated frequency noise between the fundamental and the second harmonic. The beam from a 2 W non-planar ring laser at 1064 nm is passed through a spatial filter cavity [12]. The spatially filtered beam then enters the Mach-Zehnder through a hole in an acoustic enclosure. PPKTP crystals (Raicol Crystals) inside temperature stabilized ovens are placed in each arm, with lenses added to mode match to the each crystal. Two additional dichroic mirrors (M3, M4) are placed in one arm for alignment. The beams recombine on a dichroic 50:50 beamsplitter and low loss HR mirrors ($T < 10$ ppm at 1064 nm) are used to separate the fundamental from the second harmonic. Commercial dichroic mirrors (HR532, AR1064) were used to further separate the 532 nm from the 1064 nm light. For the 532 nm and 1064 nm detection, Si (Hamamatsu 1223) and InGaAs (GPD 2000) photodiodes were used, respectively. The Mach-Zehnder arm lengths were adjusted to be mid fringe for both 532 and 1064 nm simultaneously. The interferometer is locked to this point by applying feedback from the 1064 nm PD difference signal to the PZT on M1 (see Fig. 1). We drove the PZT with a small signal at 100 Hz to monitor the calibration (rad/V) at both wavelengths, as any differential frequency noise between the two wavelengths would cause the 532 nm calibration to drift. The calibration of the Mach Zehnder was confirmed by sweeping through multiple fringes. The 1064 nm and 532 nm Mach-Zehnder length signals were read out with two pairs of balanced homodyne detectors. The sum and difference signals were digitized at 256 Hz and

processed further offline.

In the non-depleted pump approximation, with imperfect phase matching, the phase relation of the two fields in each arm before the recombining beamsplitter is:

$$\theta_{532} = 2\theta_{1064} - \pi/2 - \Delta kL/2\,, \tag{1}$$

where θ_{1064} and θ_{532} describe the relative phases of the fundamental and the second harmonic, respectively, L is the length of the doubling crystal, and Δk is the phase mismatch, the parameter normally used to describe the efficiency of SHG. In theory, Δk can be arbitrarily small (limited in practice only by the ability to stabilize the temperature of the nonlinear crystal).

Using superscripts to differentiate between the two arms, the difference in the second harmonic phase is thus

$$\theta^A_{532} - \theta^B_{532} = 2\left(\theta^A_{1064} - \theta^B_{1064}\right) - \left(\Delta k^A - \Delta k^B\right) L/2\,. \tag{2}$$

3. Results

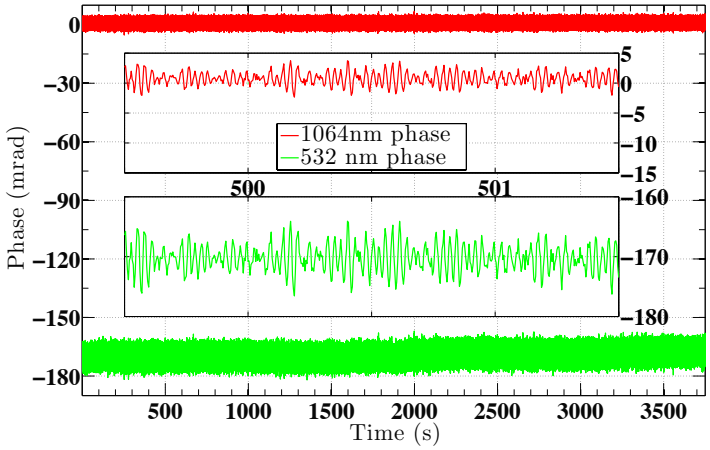

Fig. 2. Example time series of the Mach-Zehnder output. The RMS phase noise over the one hour period was 6 mrad RMS at 532 nm and 3 mrad RMS at 1064 nm

The phase difference ($\delta\theta_{1064}(t) \equiv \theta^A_{1064}(t) - \theta^B_{1064}(t)$) was suppressed by the servo, which had a unity gain frequency of $\sim$ 10 Hz. Typical values of $\delta\theta_{1064}(t)$ and $\delta\theta_{532}(t)$ are shown in Fig. 2.

The frequency noise amplitude spectral density of the Mach Zehnder is shown in Fig. 3 with known noise sources. $\delta\nu_{1064}$ and $\delta\nu_{532}$ are shown in red and green, respectively, where $\delta\nu \equiv \delta\dot{\theta}/2\pi$. Above 10 Hz the phase noise is dominated by a forest of mechanical resonances on the optical table which show up strongly in both $\delta\nu_{1064}$ and $\delta\nu_{532}$. We used the average transfer function over the measurement time, $\mathrm{H}(f) = \langle\delta\nu_{532}(f)/\delta\nu_{1064}(f)\rangle$, to subtract the noise which is coherent between the two $\delta\nu$s. This subtracted level is shown as the black trace in Fig. 3. The black trace bounds any noise source which causes frequency noise between the fundamental and the harmonic and is uncorrelated between the two ovens, such as thermodynamic fluctuations in the crystals, or any temperature fluctuation not common to both ovens. Some common mode effects such as intensity dependent phase shifts and temperature fluctuations (and thus phase matching fluctuations) are suppressed by the experimental setup, so these technical noise sources will not be visible in these measurements. However, a pessimistic estimate of the temperature noise coupling assuming no common mode rejection shown in Fig. 3

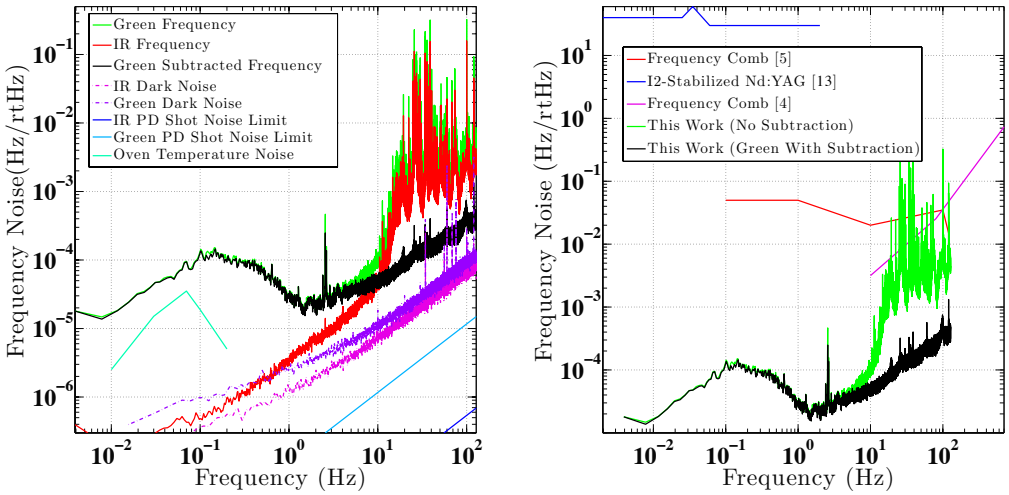

Fig. 3. On the left we see the full noise budget of the experiment: $\theta^A_{1064} - \theta^B_{1064}$ (in red) (which is the in-loop signal of the Mach-Zehnder), $\theta^A_{532} - \theta^B_{532}$ (in green) (which contains excess phase noise), and the subtraction residual (in black). The total RMS frequency fluctuation in the measurement band is 3 mHz. On the right we have a comparison of this work with previous bounds. These bounds show up as frequency noise [13], timing error [5], and phase noise [4].

is below the measured excess frequency noise. In addition, the intensity of the fundamental was only stabilized to a level of 2×10^{-6} at 1 Hz, where it can be lowered to the 10^{-8} at 1 Hz with current techniques, so unless the rejection of this effect was more than 46 dB, we can safely ignore it. It is highly improbable that the intensity to frequency noise coupling would be above the level shown in Fig. 3. The excess noise below 10 Hz was found to be correlated with air currents on the table, and would be reduced by moving the setup into a vacuum chamber. The total RMS excess frequency noise of the black trace is 3 mHz RMS in the 10 mHz to 128 Hz band.

4. Noise Sources

In addition to the usual technical noise sources, it is worth considering whether there is a more fundamental limit to the relative phase between the fundamental and the harmonic. A rough estimate of thermal noise from thermoelastic (Zener) damping was obtained by directly applying [14] the Fluctuation-Dissipation Theorem. We treat the crystal as an 0.8 mm radius cylinder, and follow the calculation done by Heinert et al. [15]. This yields a spectral density of Δk taking into account both thermorefractive and thermoelastic fluctuations. When expressed as frequency fluctuations, it is well approximated by $2.5/(1+500f^{-7/8})\,\mu\text{Hz}/\sqrt{\text{Hz}}$ above 10 Hz. Below that, it must be flat or continue to decrease, or else the RMS temperature integral would diverge. Practically speaking, in our band of interest, the temperature fluctuations of the ovens is at least 2 orders of magnitude greater than these fundamental thermodynamic temperature fluctuation. In the future, when researchers seek to make frequency comparisons at better than the 10^{-21} level, these thermal noises will have to be calculated with more accuracy.

5. Previous Bounds on Excess Frequency Noise

We have examined the results from a number of precision experiments which involve SHG. Although these experiments are likely limited by other noise sources, these data can be used to place upper bounds on the possible noise generated by SHG. In Fig. 3 we compare frequency noise [13], timing errors [5], and phase noise [4]; in Fig. 4 we compare Allan deviations [2, 3, 5, 6, 16, 17, 18]. While the comparison in Fig. 3 is straightforward, some caution should be taken interpreting Fig. 4. Our Allan deviation at the 0.1 s time scale is heavily influenced by the high frequency noise in the measurement (10-128 Hz). Since we low pass the signal to acquire data at 256 Hz, we reject noise which would make the Allan deviation increase at all time scales. It should also be emphasized that we only measure relative frequency fluctuations, and that there are some common mode noise sources which the experiment is insensitive to. See [19] for more information on Allan deviations and phase noise.

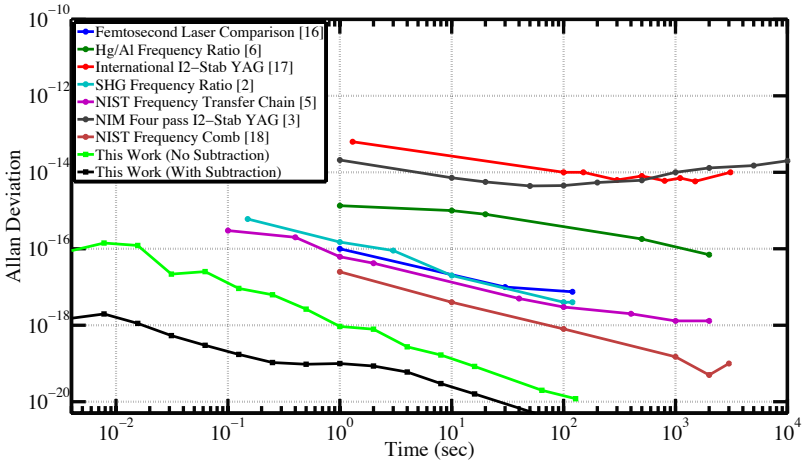

Fig. 4. The Allan deviations from this experiment (green and black) were obtained from the power spectrum as described in [20]. Bounds from previous work are shown for reference.

6. Conclusions

In conclusion, we have demonstrated that the RMS frequency fluctuations added from uncorrelated mechanisms between two SHG crystals is less than 3 mHz at time scales over 10 ms. The obvious correlated mechanisms (temperature and intensity noise coupling) are likely insignificant compared to this as discussed in section 3. This is low enough to not limit the lock acquisition [9, 10] scheme for Advanced LIGO and other gravitational-wave detectors. Additionally, we have shown that there is no excess noise process at a level which is of interest to those doing precision atomic spectroscopy [7], using frequency combs to transfer optical harmonics [4, 5, 21] and other tests of fundamental physics.

Acknowledgements

The authors would like to thank P. Fritschel for suggesting this work as well as K. Arai, J. Harms, and K. McKenzie, for discussions leading to the understanding presented in this letter, as well as H. Grote and M. Evans for useful input on the interferometer stabilization. We also gratefully acknowledge the National Science Foundation for support under grant PHY-0757058.